

Enhancing Hydrogen Storage in AZ31 Alloy through Pd/G Composite

Song-Jeng Huang¹, Chen-Ju Lai^{1,*}, Veeramanikandan Rajagopal¹, Wen-Lie Chang²

¹Department of Mechanical Engineering, National Taiwan University of Science and Technology, Taipei 10607, Taiwan

²Top Nano Technology Co., Ltd. 6F., No.11, Wuquan Rd., Wugu Township, Taipei County 248, Taiwan

Abstract: In this research, we investigated the catalytic effects of Palladium/Graphene(Pd/G) on AZ31 alloy for hydrogen storage. X-ray diffraction (XRD) analysis, scanning electron microscopy (SEM), and energy dispersive X-ray spectroscopy (SEM-EDS) were employed to confirm the homogeneous distribution of AZ31 and observe phase changes after mechanical alloying with the catalysts. The hydrogen storage properties of AZ31 with catalysts were systematically examined, and the time of maximum reaction rate for nucleation was determined using Avarami Plot. The results of the study show that the incorporation of 2% Pd/G resulted in the fastest hydrogen absorption and desorption time, taking 200 seconds to achieve 90% hydrogen storage with a maximum of 6.04 wt%. The corresponding maximum hydrogen desorption occurred in 694 seconds, reaching 6.03 wt%. Consequently, the introduction of 2% Pd/G catalyst proved to be effective in significantly enhancing the hydrogen ab/desorption rates of AZ31 alloy.

Keywords: Magnesium alloy, hydrogen storage, palladium, graphene.

1. INTRODUCTION

Hydrogen, hailed as a zero-carbon fuel, emerges as a promising alternative to traditional fossil fuels, functioning as a renewable energy carrier boasting a remarkable energy density of up to 142 MJ kg⁻¹ [1]. Its ecological impact is minimal, undergoing complete conversion into water after use [2]. This environmentally friendly attribute, coupled with hydrogen's versatility in transforming into various energy forms, positions it as an exemplary candidate for renewable energy storage [3]. The advancement of the hydrogen industry hinges on the triumvirate of low-cost production, efficient storage systems, and cutting-edge application technologies. Within this realm, efficient hydrogen storage stands out as a pivotal challenge.

Among solid hydrogen storage materials, the MgH₂/Mg system emerges as a frontrunner, showcasing high hydrogen storage density (7.6% by mass and 110 kg m⁻³ H₂ by volume), cost-effectiveness, and the abundance of magnesium, ranked as the 8th most prevalent element in the Earth's crust [4-6].

However, practical applications of magnesium-based hydrogen storage materials encounter significant obstacles. First, the thermodynamically stable enthalpy

change of hydrogen release for MgH₂ ($\Delta H=75 \text{ kJ mol}^{-1}$) poses a challenge. Second, the hydrogen absorption/release kinetics of the Mg/MgH₂ system exhibit sluggishness at temperatures below 300°C. Third, the hydrogen absorption/release cycle leads to the agglomeration and growth of MgH₂/Mg particles, compromising cyclic stability [7-9]. Addressing these challenges is imperative for unlocking the full potential of magnesium-based hydrogen storage systems.

The sluggish kinetics of magnesium (Mg) storage for hydrogen gas is predominantly attributed to the lack of interaction with the antibonding molecular orbital (σ^*) of hydrogen, crucial for promoting hydrogen molecule dissociation [10, 11]. Therefore, a catalyst that facilitates the rapid and efficient dissociation of H₂ molecules is pivotal. This process typically involves heterogeneous catalysis, highlighting the critical importance of optimizing the interaction between the catalyst and Mg [12].

Carbon nanomaterials have been utilized in many ways in recent years to enhance the mechanical, electrical, thermal and barrier properties of polymers due to their excellent physical or chemical properties, and many researchers have used carbon-based materials as reinforcement materials for various types of polymers [13, 14]. Even in recent hydrogen research, the high specific surface area, abundance of reaction sites, and excellent thermal conductivity of carbon-based materials make them a good choice for hydrogen storage, as they can increase electron

*Address correspondence to this author at the Department of Mechanical Engineering, National Taiwan University of Science and Technology, Taipei 10607, Taiwan; E-mail: lainelsonking@gmail.com

transfer and improve the kinetics of the hydrogen cycle [15].

2. EXPERIMENTAL

2.1. Material

In this investigation, the magnesium-based alloy AZ31, procured from Kuangyue Technology (Linyi) Co., served as the primary material. The catalysts employed in this study for the magnesium-based alloy AZ31 is composite of Palladium and Graphene (Pd/G).

The synthesis of Pd/G involved a reduction reaction between Palladium hydroxide ($\text{Pd}(\text{OH})_2$) and formic acid (HCOOH), resulting in the formation of nanoscale palladium metal particles, carbon dioxide, and water. These nanoscale palladium metal particles exhibited an affinity for the surface of each graphene material piece. Consequently, the influence of electrostatic repulsion caused the dispersed graphene to coalesce, facilitated by the attachment of nanoscale palladium metal particles to the graphene material surfaces.

2.2. Composite Preparation

The Palladium/Graphene composite (Pd/G) were incorporated as catalysts into AZ31 at a concentration of 2 wt.%. The AZ31 chips underwent grinding and blending with the catalysts through mechanical alloying, employing a table-top planetary ball mill PM100. The experimental parameters were established with a grinding speed set at 400 RPM, a grinding duration of 10 hours, and a ball-to-powder ratio of 1:40. High-energy ball milling was employed to ensure the homogeneous integration of AZ31 powder with the specified catalysts.

2.3. Structure Characterization

The phase compositions and transformations of the prepared powder samples were examined using X-Ray

diffraction (XRD) with a D2 phaser instrument from Bruker. A Cu-K α ray source was fixed at a voltage of 45 kV, and the current rating was set at 0.8 mA. The Bruker-EVA software was employed to analyze and identify the various phase compositions.

For morphological research and elemental composition mapping, a scanning electron microscope (SEM) equipped with an energy dispersive X-ray spectroscopy (EDS) detector, specifically model JSM-6390 L, was utilized.

2.4. Hydrogen Storage Property Measurements

To determine the hydrogen storage properties of the powder samples by Sievert's type apparatus set up by JNP TECH CO., LTD., all samples weighed 0.3 g. Oxygen was removed from the samples by vacuum for 1 hour at an initial pressure of 3.5 Mpa and 20 cycles at 375°C. The samples were then subjected to a ab/desorption cycle to determine the hydrodynamic curves of the samples. The initial pressure was set at 3.5 Mpa and 20 cycles were performed at 375°C to measure the kinetic curve of hydrogen absorption and desorption.

3. RESULT AND DISCUSSION

3.1. Material Characterization

As depicted in Figure 1a, the Pd/G powder exhibits a flake-like structure. The X-ray diffraction (XRD) pattern in Figure 2 illustrates that the carbon phase predominates in Pd/G, with the main peak attributed to carbon, followed by palladium. This observation indicates carbon as the predominant element, and the uniform distribution of palladium within the carbon matrix is confirmed through energy dispersive X-ray spectroscopy (EDS) mapping.

In Figure 3a, SEM images of 2% Pd/G mechanically alloyed with AZ31 powder via ball milling at 100x

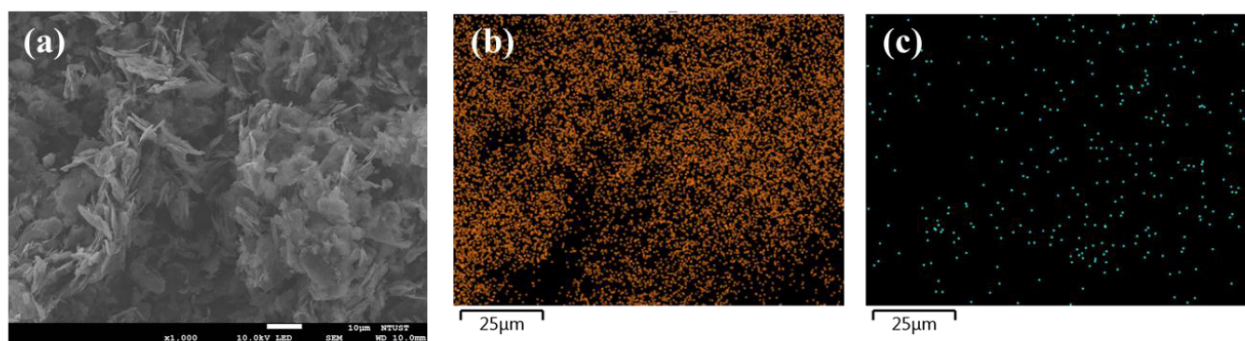


Figure 1: SEM images of (a) Pd/G. EDS mapping of (b) carbon distribution (c) palladium distribution.

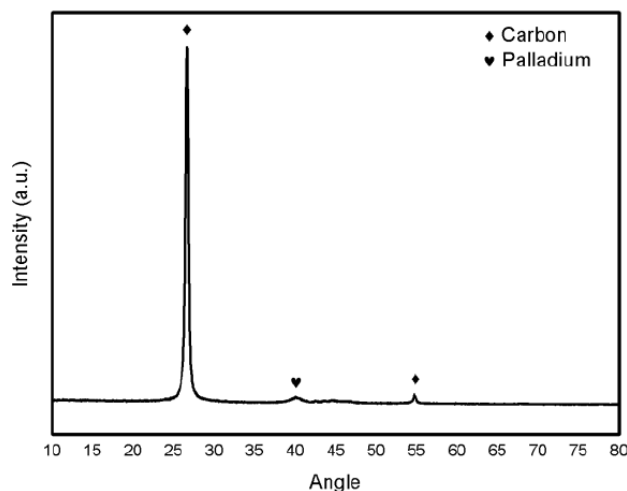


Figure 2: XRD pattern of Pd/G.

magnification are presented. The primary element in AZ31-2% Pd/G is magnesium, while zinc and manganese are elements inherent in the original AZ31

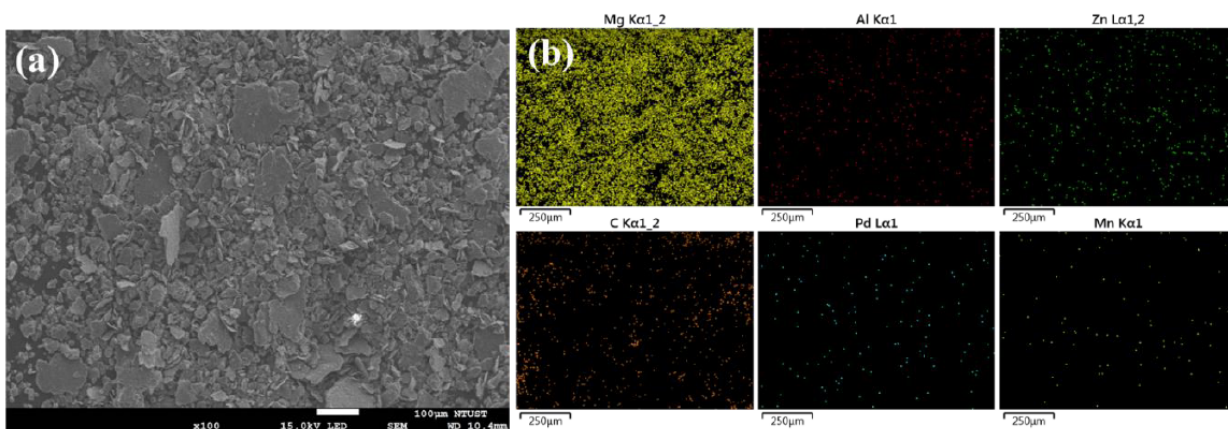


Figure 3: SEM images of AZ31-2% Pd/G (a) in 100 magnifications. (b) EDS mapping of AZ31-3%Pd/G.

powder. Notably, carbon and palladium are uniformly dispersed in AZ31 after the mechanical alloying process.

The X-ray diffraction (XRD) pattern of AZ31-2% Pd/G, illustrated in Figure 4, showcases the highest peak corresponding to the main phase $Mg_{0.97}Zn_{0.03}$, with the carbon phase exhibiting a lower intensity. The addition of 2% Pd/G introduces this carbon phase, reflecting the higher carbon content inherent in the Pd/G catalyst.

Figure 5 presents the X-ray diffraction (XRD) patterns of pure AZ31 powder and AZ31-2% Pd/G before and after hydrogen absorption, respectively. In Figure 5a, it is evident that the pure AZ31, without any treatment, still exhibits a strong peak corresponding to the $Mg_{0.97}Zn_{0.03}$ phase after hydrogen absorption. This

implies that the pure AZ31 is hard to transform the $Mg_{0.97}Zn_{0.03}$ phase into the MgH_2 phase post-hydrogen absorption. However, upon the addition of the 2% Pd/G catalyst, effective conversion of the $Mg_{0.97}Zn_{0.03}$ phase to the MgH_2 phase is achieved.

3.2. Hydrogenation Properties

In Figure 6, a comparison of hydrogen absorption and desorption among pure AZ31 with catalysts and without catalysts is presented. In Figure 6a, it is evident that AZ31 with catalysts exhibits higher hydrogen absorption and desorption rates compared to that without catalysts. The incorporation of 2% Pd/G achieved maximum hydrogen storage capacities of 6.04 wt%. Notably, 90% of the maximum hydrogen storage capacity was reached in 200 seconds with 2% Pd/G, surpassing the performance of pure AZ31, which took 1,156 seconds to reach the same threshold.

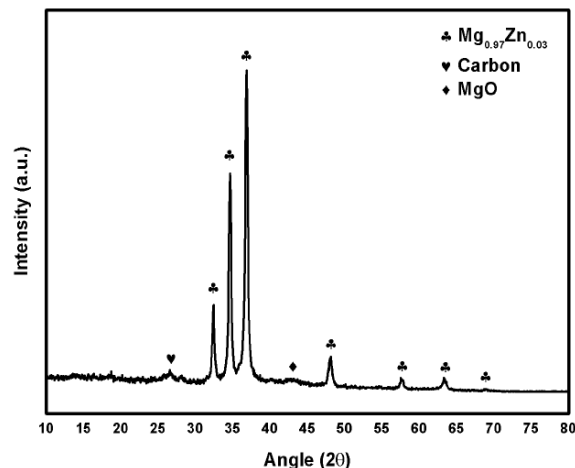


Figure 4: XRD pattern of AZ31-2% Pd/G.

In Figure 6b, it is observed that pure AZ31 without a catalyst released only 4.02 wt% of hydrogen, taking

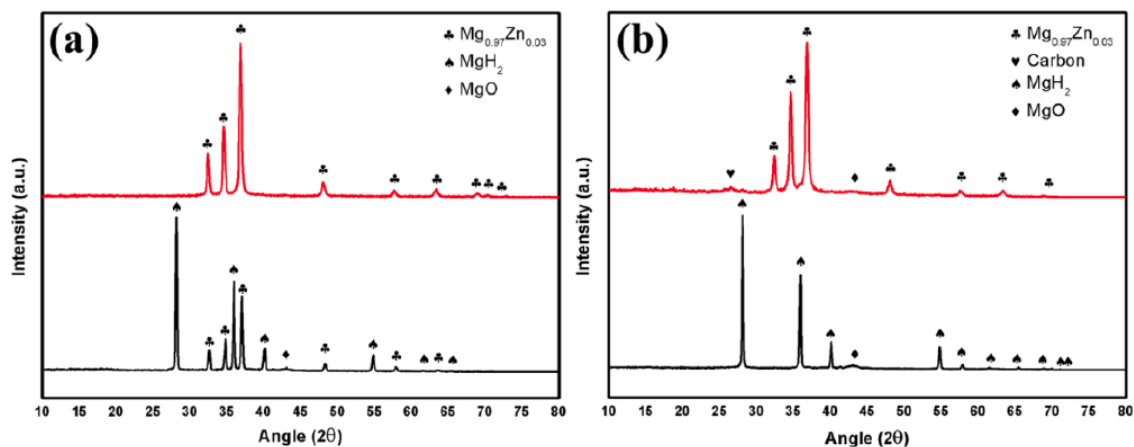


Figure 5: XRD patterns of As-AZ31 (a) and AZ31-2% Pd/G (b) before and after hydrogen absorption.

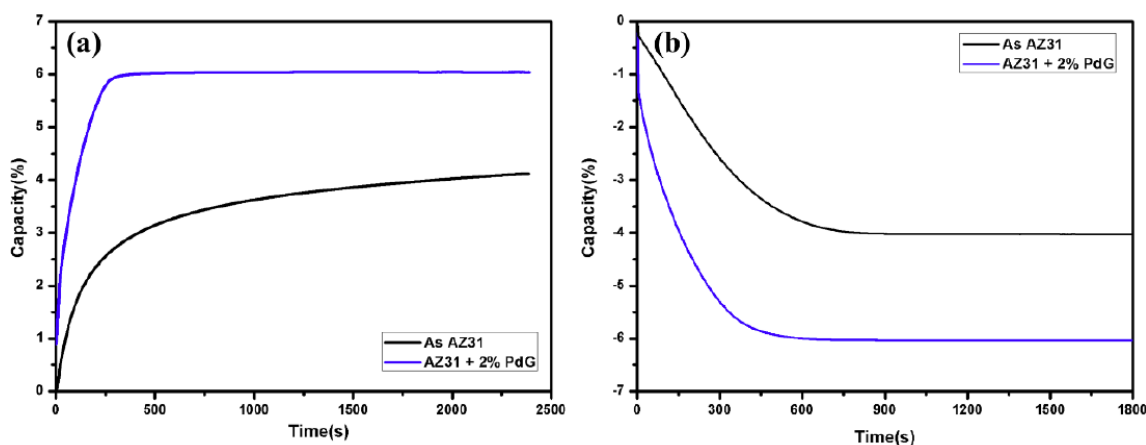


Figure 6: Absorption-desorption kinetic curves for As AZ31 (a) and AZ31-2%Pd/G (b).

966 seconds to reach the maximum hydrogen release. With 2% Pd/G, 6.03 wt% of hydrogen were released, achieving maximum hydrogen release in 694 seconds.

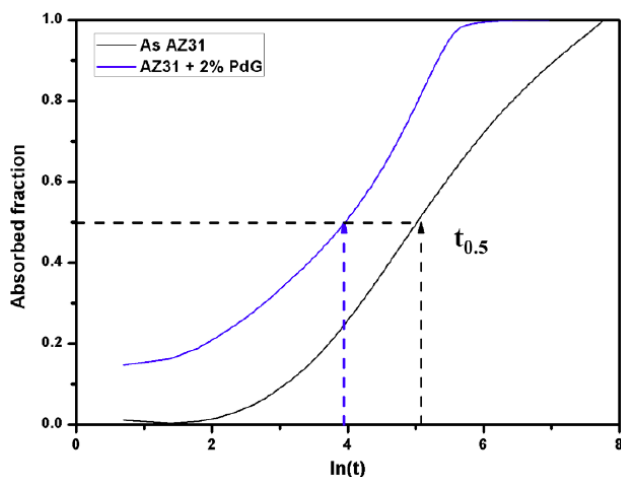


Figure 7: Avrami plots for As AZ31 and AZ31-2%Pd/G.

Utilizing the experimental data, the proportion of magnesium hydrogenated through magnesium

conversion at each time interval was plotted to generate the Avrami plot, as depicted in Figure 7. The Avrami plot illustrates the conversion rate reaching 1/2, that is, there is the maximum reaction rate at $t_{0.5}$ [16]. In Figure 7, it is evident that AZ31-2% Pd/G achieves the maximum reaction rate more rapidly than the pure AZ31, exhibiting a significant advantage over pure AZ31 without a catalyst.

The introduction of catalysts has proven to be efficacious in elevating the nucleation point for the conversion of magnesium to magnesium hydride, as demonstrated in prior research [17]. This observed trend can be attributed to the fact that 2% Pd/G provides ample nucleation points, effectively accelerating the rate of magnesium conversion to magnesium hydride.

4. CONCLUSION

This study investigated the catalytic effects of Pd/G on AZ31, employing X-ray diffraction (XRD) analysis,

scanning electron microscopy (SEM), and energy dispersive X-ray spectroscopy (SEM-EDS) to confirm the homogeneous distribution of AZ31 and observe phase changes post-mechanical alloying with the catalysts. Additionally, the hydrogen storage properties of AZ31 with catalysts were systematically examined, and the Avrami Plot was employed to determine the time of the maximum reaction rate for nucleation.

The results revealed that the incorporation of 2% Pd/G exhibited the swiftest hydrogen absorption and desorption times. It took 200 seconds to achieve 90% hydrogen storage, reaching a maximum storage capacity of 6.04 wt%, and 694 seconds to attain a maximum hydrogen desorption of 6.03 wt%. Therefore, the introduction of 2% Pd/G catalyst effectively enhances the hydrogen ab/desorption rates of AZ31.

DECLARATION OF INTEREST STATEMENT

The authors declare that there isn't any conflict of interest with regard to the current study.

ACKNOWLEDGEMENT

The authors extend their appreciation to the National Science and Technology Council, Taiwan, for their financial support in the form of project grant number NSTC 111-2221-E-011-096-MY3.

REFERENCES

- [1] Schlapbach L, Züttel A. Hydrogen-storage materials for mobile applications. *Nature* 2001; 414: 353-358. <https://doi.org/10.1038/35104634>
- [2] Sadhasivam T, Kim H-T, Jung S, Roh S-H, Park J-H, Jung H-Y. Dimensional effects of nanostructured Mg/MgH₂ for hydrogen storage applications: A review. *Renewable and Sustainable Energy Reviews* 2017; 72: Pages 523-534, ISSN 1364-0321. <https://doi.org/10.1016/j.rser.2017.01.107>
- [3] Wang H, Lin HJ, Cai WT, Ouyang LZ, Zhu M. Tuning kinetics and thermodynamics of hydrogen storage in light metal element based systems – A review of recent progress. *Journal of Alloys and Compounds* 2016; 658: 280-300. ISSN 0925-8388, <https://doi.org/10.1016/j.jallcom.2015.10.090>
- [4] Lai Q, Paskevicius M, Sheppard DA, Buckley CE, Thornton AW, Hill MR, Gu Q, Mao J, Huang Z, Liu HK, Guo Z, Banerjee A, Chakraborty S, Ahuja R, Aguey-Zinsou K-F. Hydrogen Storage Materials for Mobile and Stationary Applications: Current State of the Art. *ChemSusChem* 2015; 8: 2789-2825. <https://doi.org/10.1002/cssc.201500231>
- [5] Bardhan R, Ruminiski AM, Brand A. Magnesium nanocrystal-polymer composites: A new platform for designer hydrogen storage materials. *Energy Environ Sci* 2011; 4: 4882-4895.
- [6] Pistidda C, Bergemann N, Wurr J. Hydrogen storage systems from waste Mg alloys. *J Power Sources* 2014; 270: 554-563.
- [7] Chen H, Yu H, Zhang Q. Enhancement in dehydrogenation performance of magnesium hydride by iron incorporation: A combined experimental and theoretical investigation. *J Power Sources* 2016; 322: 179-186.
- [8] Chen H, Han Z, Feng X. Solid-phase hydrogen in a magnesium-carbon composite for efficient hydrogenation of carbon disulfide. *J Mater Chem A* 2018; 6: 3055-3062.
- [9] Zhang Q, Du S, Ma Z, Lin X, Zou J, Zhu W, Ren L, Li Y. Recent advances in Mg-based hydrogen storage materials. *Chinese Science Bulletin* 2022; 67(19): Pages 2158-2171, ISSN 0023-074X
- [10] Kecik D, Aydinol MK. Density functional and dynamics study of the dissociative adsorption of hydrogen on Mg (0001) surface. *Surface Science* 2009; 603(2): 304-310, ISSN 0039-6028. <https://doi.org/10.1016/j.susc.2008.11.017>
- [11] Christmann K. Some general aspects of hydrogen chemisorption on metal surfaces. *Progress in Surface Science* 1995; 48(1-4): 15-26, ISSN 0079-6816
- [12] Yang Y, Zhang X, Zhang L, Zhang W, Liu H, Huang Z, Yang L, Gu C, Sun W, Gao M, Liu Y, Pan H. Recent advances in catalyst-modified Mg-based hydrogen storage materials. *Journal of Materials Science & Technology* 2023; ISSN 1005-0302.
- [13] Hussein AH, *et al.* Graphene-reinforced polymer matrix composites fabricated by in situ shear exfoliation of graphite in polymer solution: processing, rheology, microstructure, and properties. *Nanotechnology* 2021; 32(17): 175703. <https://doi.org/10.1088/1361-6528/abd359>
- [14] Mittal G, Dhand V, Rhee KY, Park S-J, Lee WR. A review on carbon nanotubes and graphene as fillers in reinforced polymer nanocomposites. *Journal of Industrial and Engineering Chemistry* 2015; 21: 11-25. <https://doi.org/10.1016/j.jiec.2014.03.022>
- [15] Yang Y, Zhang X, Zhang L, Zhang W, Liu H, Huang Z, Yang L, Gu C, Sun W, Gao M, Liu Y, Pan H. Recent advances in catalyst-modified Mg-based hydrogen storage materials. *Journal of Materials Science & Technology* 2023; 163: 182-211, ISSN 1005-0302. <https://doi.org/10.1016/j.jmst.2023.03.063>
- [16] Faleiros A, Rabelo TN, Thim G, Oliveira M. Kinetics of Phase Change. *Materials Research* 2000; 3: 10.1590/S1516-14392000000300002.
- [17] Salman, Saad M, *et al.* Catalysis in Solid Hydrogen Storage: Recent Advances, Challenges, and Perspectives. *Energy Technology* 2022; 10(9): 2200433.

Received on 20-09-2023

Accepted on 20-10-2023

Published on 28-11-2023

<https://doi.org/10.6000/1929-5995.2023.12.18>

© 2023 Huang *et al.*; Licensee Lifescience Global.

This is an open-access article licensed under the terms of the Creative Commons Attribution License (<http://creativecommons.org/licenses/by/4.0/>), which permits unrestricted use, distribution, and reproduction in any medium, provided the work is properly cited.